

Air-sea heat fluxes associated to mesoscale eddies in the Southwestern Atlantic Ocean and their dependence on different regional conditions

Inés M. Leyba¹ · Martín Saraceno¹ · Silvina A. Solman¹

Received: 5 April 2016 / Accepted: 15 November 2016 / Published online: 28 November 2016
© Springer-Verlag Berlin Heidelberg 2016

Abstract Heat fluxes between the ocean and the atmosphere largely represent the link between the two media. A possible mechanism of interaction is generated by mesoscale ocean eddies. In this work we evaluate if eddies in Southwestern Atlantic (SWA) Ocean may significantly affect flows between the ocean and the atmosphere. Atmospheric conditions associated with eddies were examined using data of sea surface temperature (SST), sensible (SHF) and latent heat flux (LHF) from NCEP–CFSR reanalysis. On average, we found that NCEP–CFSR reanalysis adequately reflects the variability expected from eddies in the SWA, considering the classical eddy-pumping theory: anticyclonic (cyclonic) eddies cause maximum positive (negative) anomalies with maximum mean anomalies of 0.5 °C (−0.5 °C) in SST, 6 W/m² (−4 W/m²) in SHF and 12 W/m² (−9 W/m²) in LHF. However, a regional dependence of heat fluxes associated to mesoscale cyclonic eddies was found: in the turbulent Brazil–Malvinas Confluence (BMC) region they are related with positive heat flux anomaly (ocean heat loss), while in the rest of the SWA they behave as expected (ocean heat gain). We argue that eddy-pumping do not cool enough the center of the cyclonic eddies in the BMC region simply because most of them trapped very warm waters when they originate in the subtropics. The article therefore concludes that in the SWA: (1) a robust link exists between the SST anomalies generated by eddies and the local anomalous heat flow between the ocean and the atmosphere; (2)

in the BMC region cyclonic eddies are related with positive heat anomalies, contrary to what is expected.

Keywords Mesoscale eddies · South Atlantic · Heat flux

1 Introduction

1.1 Air-sea fluxes and oceanic eddies

The ocean and the atmosphere are strongly related. The ocean is an important source of energy for the atmospheric circulation that is in turn the main forcing of the surface circulation of the ocean. Heat fluxes and wind stress represent the link between the ocean and the atmosphere. Surface turbulent heat fluxes are thus crucial to the global heat budget. The fundamental processes that connect the atmosphere with the ocean are the energy input to the ocean by the wind, the net freshwater flux and the net surface heat flux. The main heat transfer between the ocean and the atmosphere is due to turbulent heat exchange in the form of sensible and latent heat. Globally, approximately 60% of the solar radiation absorbed at the earth's surface is released by latent and sensible heat, primarily from the ocean (Trenberth et al. 2009). Such fluxes are a fundamental part of the ocean surface heat budget and they are also capable of altering the sea surface temperature (SST), wind and air specific humidity (Yu and Weller 2007), being one of the primary processes by which the ocean releases heat to the atmosphere (Cayan 1992). Mesoscale processes in the ocean play a fundamental role in regulating the Earth's climate, because of its ability to redistribute properties such as heat, salt and nutrients in the ocean (e.g. Gaube et al. 2013). Furthermore, several recent studies show that there is a strong correlation between these phenomena

✉ Inés M. Leyba
ines.leyba@cima.fcen.uba.ar

¹ Centro de Investigaciones del Mar y la Atmósfera, CONICET-Universidad de Buenos Aires, Departamento de Ciencias de la Atmósfera y los Océanos/FCEN, UMI IFAECI/CNRS, Ciudad Universitaria, Pabellón II, 2do Piso, C1428EGA Buenos Aires, Argentina

and the wind on the ocean surface (Chelton and Xie 2010; Frenger et al. 2013; Chelton 2013; Souza et al. 2014). This result implies that processes such as fronts or ocean eddies can significantly affect flows between the sea and the atmosphere (Chelton 2005). In turn, the energy input provided by the fluxes of sensible and latent heat from the ocean to the atmosphere represents a modulator mechanism of the atmosphere (Xie 2004). Thus, air-sea interaction generated by mesoscale ocean eddies represent an important coupled interaction between the ocean and the atmosphere at the sea surface. Understanding air-sea fluxes generated by eddies is therefore critically important for both oceanic and atmospheric circulations. Gain in such understanding may improve weather forecast and help determining the roles of the ocean and atmosphere in climate variability (e.g. Chelton and Xie 2010). In a recent study, Frenger et al. (2013) showed that eddies in the Southern Ocean affect the atmosphere: anticyclonic eddies (AE) of warm core are associated with increased local precipitation while in cyclonic eddies (CE) occurs the opposite. Such SST anomalies were positively correlated with anomalies in other atmospheric properties. It is also clear that the atmosphere responds to mesoscale oceanic features, such as fronts and horizontal gradients (Samelson et al. 2006). Moreover, Villas Bôas et al. (2015) found that the contribution of eddies to the surface heat flux is non-negligible: turbulent heat fluxes anomalies associated with CE (AE) are negative (positive), indicating ocean heat gain (loss). A number of studies dedicated to understand the signature of oceanic mesoscale eddies have also shown that eddies leave a different imprint on overlying wind, cloud coverage and rain (e.g. Hausmann and Czaja 2012; Souza et al. 2014; Byrne et al. 2015).

Although mesoscale eddies are known to impact the ocean surface and the overlying atmospheric boundary layer, the study of their role on the heat exchange at the air-sea interface is incipient. This work explores the influence of eddies on the atmosphere, considering the Southwestern Atlantic Ocean as a case of study. The hypothesis is that polarity and other characteristics of eddies can significantly affect the fluxes between the ocean and atmosphere. The validation of this hypothesis will improve the understanding of the role that eddies have on the atmosphere in this particularly complex region.

1.2 The Southwestern Atlantic Ocean circulation and eddy distribution

The Southwestern Atlantic (SWA) ocean is populated by a large number of eddies (e.g. Saraceno and Provost 2012). This feature is due to the strong mesoscale activity that is generated as a result of the confluence of the Brazil and

Malvinas currents. In fact, the collision between the two currents at approximately 38°S makes this region one of the most energetic of the world ocean (e.g. Gordon 1981; Chelton et al. 1990). The Malvinas Current is part of the northern branch of the Antarctic Circumpolar Current that carries the cold and relatively fresh subantarctic water (Piola and Gordon 1989). The Brazil Current flows poleward along the continental margin of South America as part of the western boundary current of the South Atlantic subtropical gyre. Two main oceanic fronts are present in the SWA: the Subantarctic Front and the Brazil Current Front. The former is the northern boundary of subantarctic water and the latter is the southern limit of the South Atlantic Central Water. Another unique feature of the SWA is the presence of a large anticyclonic circulation centered at 45°S–45°W. This circulation is caused by the presence of a zonal sedimentary elevation known as Zapiola ridge. The effect of this topographic feature on the ocean surface is clearly seen in satellite images of SST, chlorophyll-a and sea surface height (Saraceno et al. 2009; Saraceno and Provost 2012). A scheme of the upper circulation of the region, including the position of the fronts, is shown in Fig. 1.

This paper is organized as follows: data and methodologies used are presented in Sect. 2. In Sect. 3 results are presented in two sub-sections: Sect. 3.1 deals with characterizations of mesoscale eddies in the SWA while Sect. 3.2 presents the results from a regional analysis. Finally, a summary of the results and main conclusions are discussed in Sect. 4.

2 Data and methods

2.1 Satellite altimetry and eddies dataset

Several methods to identify mesoscale eddies from sea level anomaly maps have been developed and broadly used in recent years. These methods rely either on physical or geometrical properties of the flow field. We use the global dataset of mesoscale eddies available at www.cioos.coas.oregonstate.edu/eddies/ (Chelton et al. 2011). In that database, eddies are obtained by an automated algorithm by identifying closed contours in spatially high-pass filtered sea surface height fields in Version 3 of the AVISO Reference Series. Only eddies with lifetimes of at least 4 weeks and amplitudes of at least 1 cm are retained (Chelton et al. 2011). From the global database, we considered eddies in the region 32–70°W, 32–53°S, that were in waters deeper than 300 m and that were identified between October 1992 and December 2010, which is the time period coincident with the dataset used to estimate the influence of eddies on the atmosphere described below.

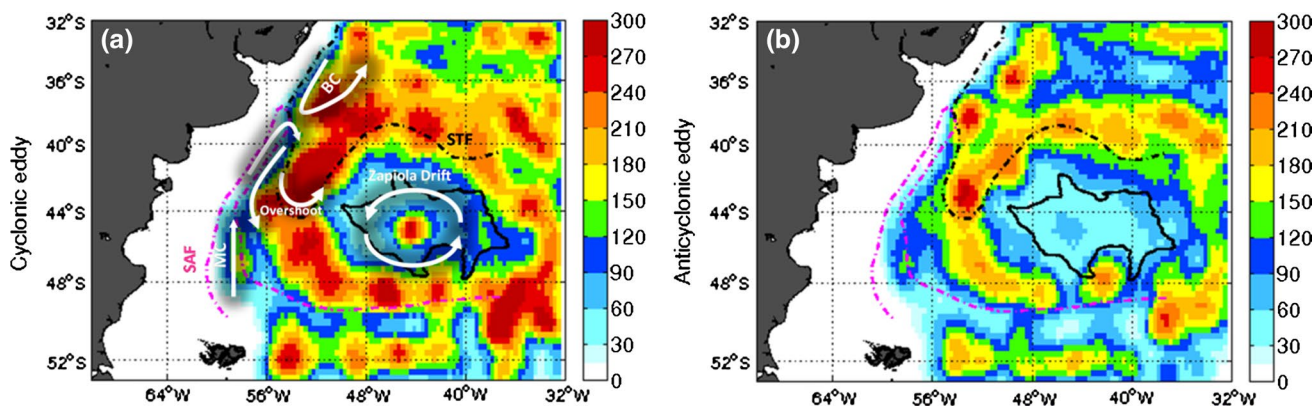


Fig. 1 Spatial distribution of the number of **a** CE and **b** AE in the SWA. The mean positions of the Subtropical Front (STF) and the Subantarctic Front (SAF) are from Saraceno et al. (2004) (indicated by *black* and *magenta dash-dotted lines*, respectively). The *boldface* closed potential vorticity contour centred at 43.1°W, 45.1°S corre-

sponds to the $-1.92 \cdot 10^{-8} \text{ m}^{-1} \text{ s}^{-1}$ value and is used to represent the Zapiola Drift area (Saraceno et al. 2009). Representative position of the Malvinas Current (MC), Brazil Current (BC), overshoot region and Zapiola Drift are indicated with *white arrow*

2.2 Atmospheric variables

The dataset used to estimate the influence of eddies on the atmosphere was obtained from the Climate Forecast System Reanalysis, CFSR, (Saha et al. 2010) produced by the US National Centers for Environmental Prediction (NCEP). CFSR is a global, high-resolution, coupled atmosphere–ocean–land surface–sea ice model, which utilizes a suite of observational and model data. In contrast to previous reanalysis products, new features of CFSR include: 6-h guess fields from a coupled atmosphere–ocean system, interactive sea ice model, assimilation of satellite radiances over the entire period, and consideration of variations of carbon dioxide (CO_2), aerosols and other trace gases and solar activity. CFSR has an atmospheric resolution of 38 km with 64 levels from the surface to 0.26 hPa. More details about the CFSR can be found in Saha et al. (2010). In this work we used SHF, LHF and SST for the period October 1992–December 2010, with spatial grid resolution of $0.25^\circ \times 0.25^\circ$ and 6-h resolution.

Anomalies of SHF, LHF and SST were constructed by removing the observed mean state that was estimated by averaging all observations available at a given location and day of the year over the period of analysis.

2.3 Methods

The spatial distribution of the concentration of eddies was computed as the number of times an eddy was detected in each pixel. To compute the spatial distribution of the radius we average the radii of all eddies within a given pixel. This methodology was also used to construct the spatial distribution of the amplitude of eddies.

Eddies composite were constructed as in Saraceno and Provost (2012): the average of SHF, LHF and SST was computed within cyclonic and anticyclonic eddy interiors in a translating and normalized coordinate system. To compute composite maps, we first localized the geographical position of each eddy. Then, we select the field of each variable corresponding to the date of eddy detection and calculated the anomalies of SHF, LHF and SST by removing the observed mean state. For each eddy realization, the heat fluxes anomalies were interpolated to a uniform grid centered on the eddy. The extension of the normalized grid was chosen in order to represent the anomaly fields to a distance of one eddy radius in each direction. After the normalization, the anomaly fields of each eddy is represented on the normalized coordinate system as a circle of unitary radius, regardless of the original shape and size of the eddy. This normalization allows averaging the anomalies of thousands of eddies as a single composite map.

3 Results

3.1 Characterization of mesoscale eddies in the Southwestern Atlantic Ocean

We first analyze the climatology of eddies. Their main properties are consistent with the patterns described in other works in the SWA. The number of eddies (Fig. 1) is maximum in regions where the eddy kinetic energy (EKE, not shown here, please refer to Saraceno and Provost 2012) is higher, such as in the BMC region or between the SAF and the Zapiola Drift, for both polarities. The total number of CE (22,579) is larger than the number of AE (16,365) for

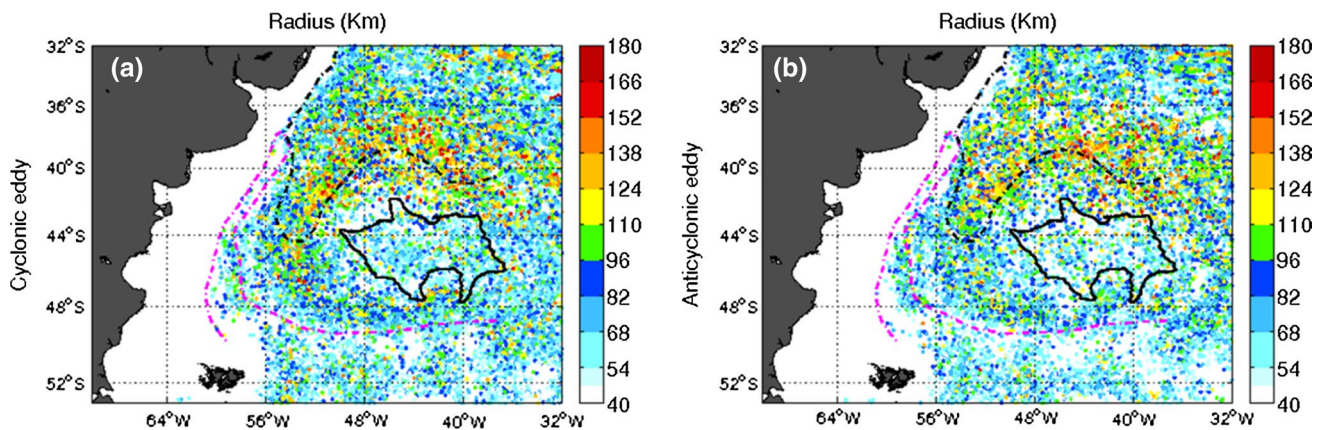


Fig. 2 Spatial distribution of the mean eddy radius (km) of **a** CE and **b** AE in the SWA. Eddies with radius lower than 40 km are masked (white)

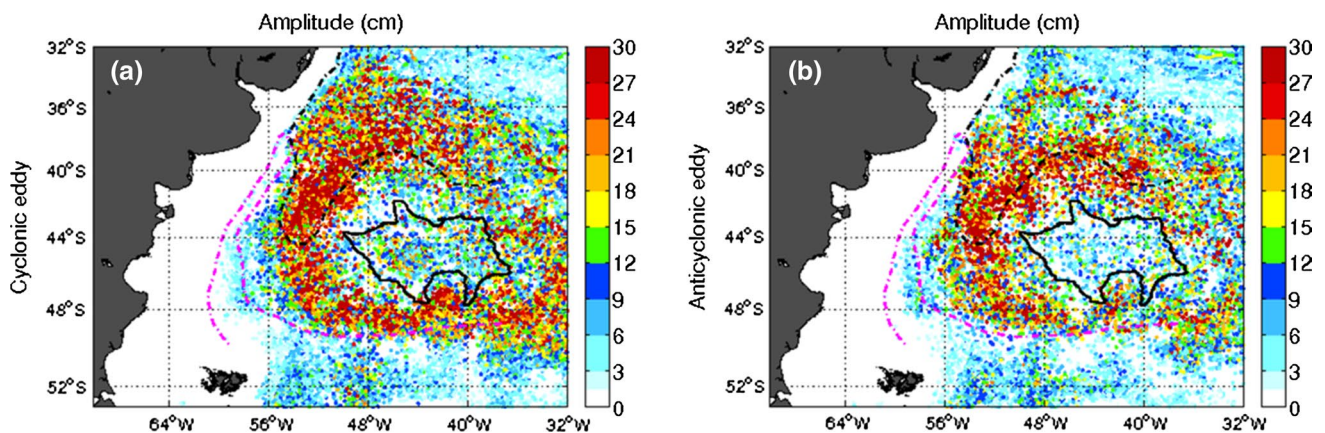


Fig. 3 Spatial distribution of the mean eddy amplitude (cm) of **a** CE and **b** AE in the SWA

the period and region considered. The spatial distribution obtained is similar to that obtained by Saraceno and Provost (2012). As observed there, the spatial distribution of eddies suggests that the main generation of eddies is produced from meanders of the currents: CE (AE) might detach from a meander of the current on the left (right) side when looking downstream on the current. Within the Zapiola anticyclone most eddies are cyclonic. Saraceno and Provost (2012) explained that in this particular region the bottom topography plays a key role in determining the polarity of eddies that might enter this region: CE generate from meanders of the large Zapiola anticyclone current and enter the region through the northeastern border, where the gradient of potential vorticity is lower. We finally observe here that south of the SAF and west of 40°W both CE and AE display a relative minimum and then concentrate into three local maximums. Detailed comparison with the bathymetry (not shown) suggests that the three maxima correspond to the main passages of the Antarctic Circumpolar Current to

the South Atlantic, i.e. west and east of Burdwood Bank and Shark Rock Passage. The relative minimum between the SAF and these passages suggests that there are few eddies that connect the SWA with the southern ocean.

The spatial distribution of the radius for CE and AE is depicted in Fig. 2. Eddies with radius larger than 150 km are located in the BMC and south of the STF. There are no significant differences between the spatial distributions of cyclonic and anticyclonic eddies as a function of their radius. The median of the radii of AE is 66 km and for CE is 61 km. For the two eddy polarities, the mean value of the radius is 82 km. The geographical distribution of the mean eddy radius is characterized by a decrease from about 150 km in the low-latitude regions to about 60 km at higher latitudes, which is consistent with the dependency of the baroclinic Rossby radius of deformation with the Coriolis parameter. Lowest eddy radii (40–100 km) are located south of the SAF.

The spatial distribution of the eddy amplitude (Fig. 3) matches very well the regions where the EKE is the highest.

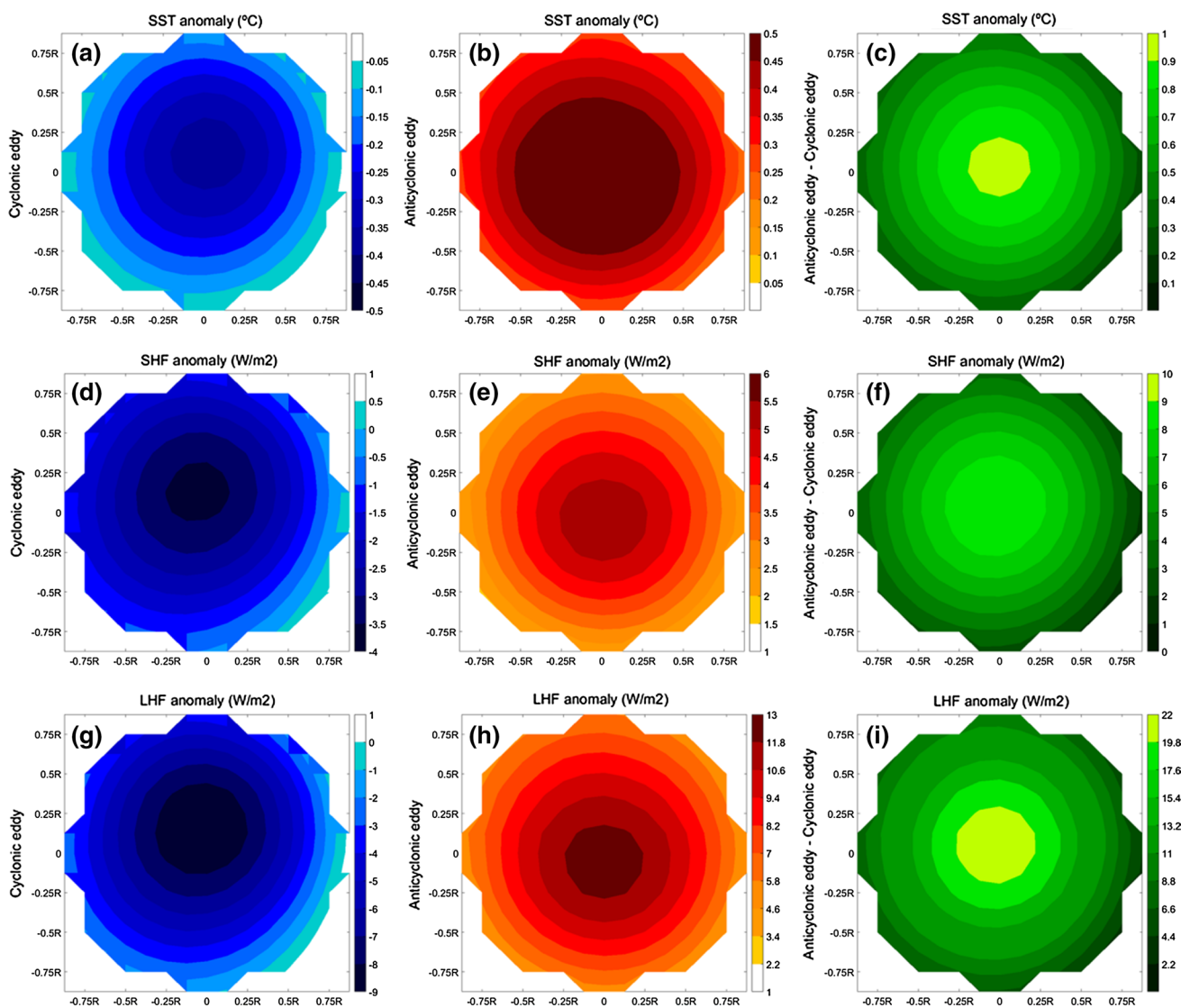


Fig. 4 Composite average of sea surface temperature (°C), sensible and latent heat flux (W/m²) inside CE and AE. Eddies are normalized and averaged from NCEP–CFSR (30 km, 6 h) for the period 1992–

2010. The zonal mean was removed. The 3th column shows the difference between AE and CE

Eddies with the largest amplitudes (>24 cm) are located in the BMC, STF and north of the SAF for both polarities. The lowest amplitudes (<9 cm) are observed south of the SAF, in the northeast corner of the region and within the Zapiola anticyclone, also for both polarities. The most frequently occurring amplitude in the whole region is of about 3 cm for both polarities. On average the mean amplitude of CE (14.55 cm) is larger than the mean amplitude of the AE (12.24 cm).

The mean composite of the imprint of eddies in the LHF, SHF and SST were computed to investigate the signature of eddy forcing on the atmosphere. Figure 4 shows the composite maps obtained for CE and AE, constructed as explained in Sect. 2 and considering all eddies detected in

the SWA in waters deeper than 300 m. Two main observations can be done here:

1. NCEP–CFSR reanalysis adequately reflects the expected variability of mesoscale eddies in SST anomaly: CE have a cold core (about −0.5 °C, Fig. 4a) while AE have a warm core (about 0.5 °C, Fig. 4b). Magnitude and spatial patterns in Fig. 4 are in agreement with results presented by Frenger et al. (2013). The classic eddy pumping is the main mechanism associated to the above-described pattern: eddies are associated with a decrease or an increase in the SST due to the vertical motions driven by relative vorticity variations, i.e. by vortex acceleration/decay (Klein and Lapeyre

2009; Frenger et al. 2013). Negative anomalies of sea level height are related to CE that rotate clockwise in the Southern Hemisphere (SH), while positive anomalies correspond to AE (counterclockwise in the SH). Eddy pumping occurs by the vertical displacement of the isopycnals producing upwelling (downwelling) and decrease (increase) of SST in the center of CE (AE); e.g. McGillicuddy and Robinson (1997), Tilburg et al. (2002). Thus, results found here and elsewhere (e.g. Frenger et al. 2013; Gaube et al. 2013, Chelton 2013) provide robust evidence that the eddy pumping mechanism plays an important role to explain the SST anomalies inside eddies in all the oceans.

The eddy pumping conceptual model explained above directly links the temporal variations of surface height anomalies to vertical motion in oceanic eddies. Still, this model is limited by the fact that only idealized circular flow-like are considered and the impact of the boundary processes are not considered (Nardelli 2013).

2. The pattern of the atmospheric imprint by oceanic eddies in SHF (Fig. 4d, e) and LHF (Fig. 4g, h) is very similar to the SST pattern (Fig. 4a, b): radially concentric and with the largest amplitude in the center of the eddy. CE have largest negative values (-4 W/m^2 for SHF and -9 W/m^2 for LHF) in the center while AE have largest positive values (6 and 12 W/m^2) in the center. The interpretation of the flux patterns is straightforward: SST anomaly produced by oceanic eddies generates air-sea disequilibrium, and therefore anomalous heat fluxes. Consequently, both sensible and latent heat flux anomalies associated with CE are negative, indicating ocean heat gain (Fig. 4d, g), while for AE are positive, indicating heat loss from the ocean to the atmosphere (Fig. 4e, h). It is important to remark that an anomaly in SST might change the SHF by modifying the temperature gradient between the ocean and the atmosphere. Also, warmer air would hold more moisture than colder air. For instance, a positive SST anomaly, as induced by AE, could lead to positive SHF/LHF anomalies, while the opposite occurs for cyclonic eddies. Thus, net surface heat fluxes (sensible and latent) clearly suggest the imprint of oceanic mesoscale eddies. Finally, Fig. 4c, f, i highlight that the amplitude of the anomalies are more intense within AE than within CE.

In order to investigate the spatial distribution of the SHF and LHF associated to eddies, we computed their net effect in the region of study (Fig. 5) following the methodology described in Sect. 2. Only significant values are plotted in Fig. 5. It is possible to observe a clear contribution from eddies to both components of the surface turbulent heat

fluxes. The geographical distribution of SHF and LHF anomalies are very similar for CE, with the highest values in the BMC (20 W/m^2 for SHF and 70 W/m^2 for LHF) and the lowest values at 40°S between 42°W and 32°W (-40 W/m^2 for SHF and -80 W/m^2 for LHF), respectively. For AE, SHF and LHF anomalies are always positive. SHF anomalies for AE range from 1.5 to 15 W/m^2 while LHF anomalies can reach values of up to 30 W/m^2 . On average, the BMC is characterized by strong heat flux anomalies, while north of 36°S and south of 50°S anomalies are weaker in CE (Fig. 5a, c) and almost no significant in AE (Fig. 5b, d). The most remarkable observation of these figures is the quite strong positive values in both SHF and LHF anomalies for CE in the BMC region (Fig. 5a, c). In general, anomalies of sensible and latent fluxes are positive in warm-core eddies and negative in cold-core eddies (e.g. Villas Bôas et al. 2015). To better characterize the BMC eddy-flux related behavior, we composite the imprint of eddies within three different regions in the next sub-section.

3.2 Sub-regional composites of SHF and LHF

We defined three regions to composite eddies (see Fig. 5a). Region I is occupied by warm subtropical waters and a moderate to low EKE; region II has cold and relatively fresh subantarctic water and moderate to large EKE; region III encompass the BMC region, where a strong mixing of cold and warm waters occurs and EKE are the highest of the region. Figures 6 and 7 show SHF and LHF eddy-composite means following the same methodology to construct Fig. 4 but for eddies identified in the three regions defined above. Anomalous SHF and LHF heat fluxes in regions I and II (Figs. 6c–f, 7c–f), for both polarities of eddies, are about half or less of the amplitude obtained considering all the eddies in the region (Fig. 4). In Region III composite of CE gives positive anomalies of latent and sensible fluxes (Figs. 6a, 7a), contrary to what is observed in the rest of the region and to what is expected following the classical eddy pumping mechanism. A possible hypothesis to explain the positive SST anomalies within CE in Region III could be that the doming of the isopycnals is not enough to cool surface waters. This is quite possible in this region since eddies that come from the North transport subtropical waters, which are very warm. An analysis of the trajectory of all CE that pass through the BMC (region III) indeed shows that 60.6% of them originate in the warm subtropical waters and propagate southward.

It is also noteworthy that the pattern distribution of the anomalies inside composites of CE and AE (Figs. 6, 7) is not symmetric. The largest amplitude of anomalies is close to the eddy center and decay radially outward. Heat flux anomalies in the SWA are larger in Region III, reaching up to 12.5 W/m^2 (28 W/m^2) in AE associated to SHF (LHF).

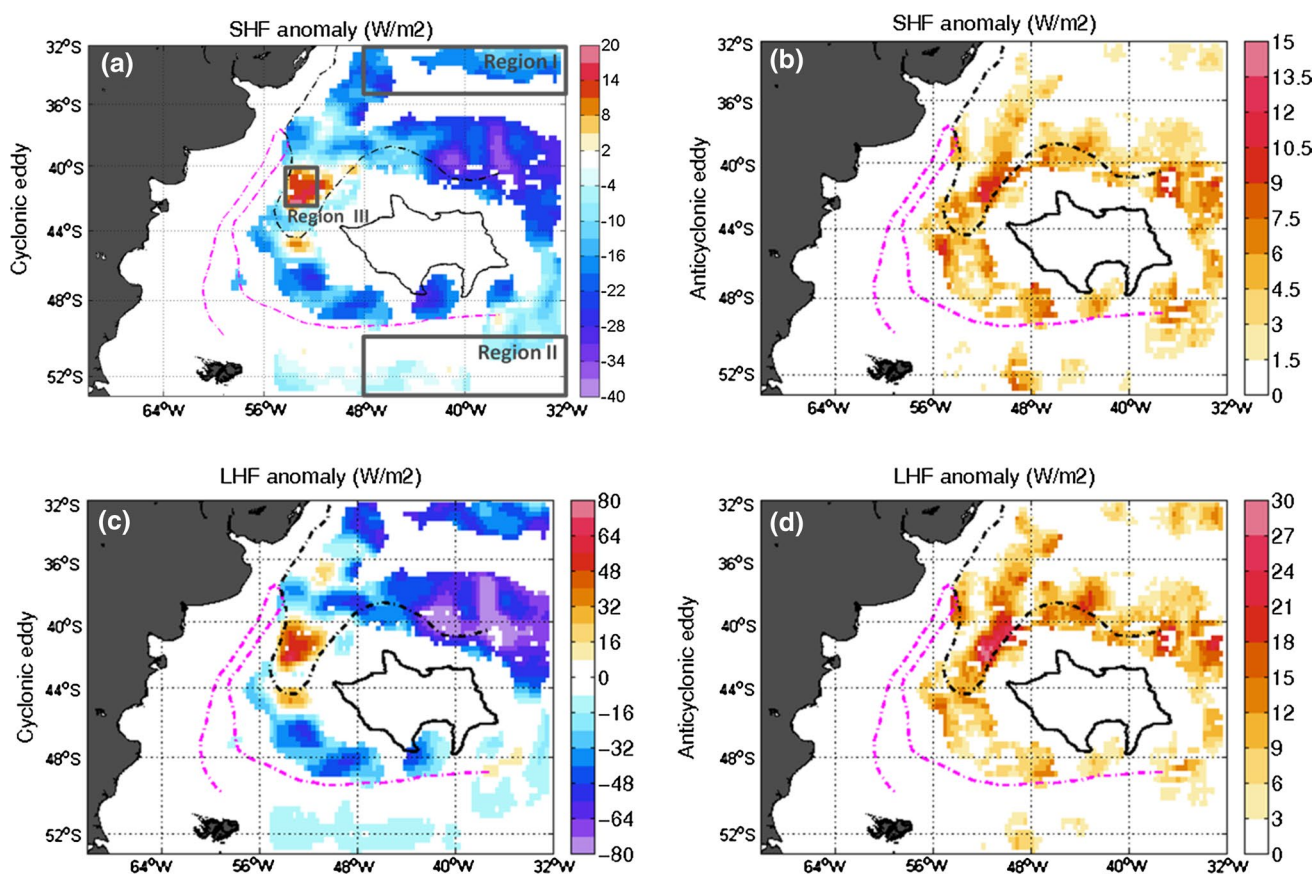


Fig. 5 Spatial distribution of sensible and latent heat flux (W/m^2) over CE (a, c) and AE (b, d) in the SWA, respectively. Regions where anomalies are less significant at the 90% confidence level and <120 eddies are masked (white)

Previous studies suggest that there is a correspondence between eddy flux behavior and eddy amplitude and radius: The larger the eddy amplitude, the stronger the SST and heat flux anomalies (Villas Bôas et al. 2015). As shown in Figs. 2 and 3 eddies with the largest amplitude and radius are located in the BMC and indeed have the highest heat flux anomalies among the SWA (Figs. 6a, b, 7a, b).

Summarizing, on average in the SWA the imprint of CE (AE) correspond to negative (positive) anomalies of SST, SHF and LHF, other authors (Villas Bôas et al. 2015) and in other regions of the ocean (e.g.; Chelton and Xie 2010; Hausmann and Czaja 2012; Gaube et al. 2013). However, careful inspection of the imprint of eddies in BMC (Region III) reveals that CE does not behave in the same way. We propose that the sign of the anomalies depends on the physical conditions of the region where eddies develop.

4 Summary and discussion of main results

The focus of the research presented here is to analyze air-sea interactions associated to mesoscale eddies in the

Southwestern Atlantic Ocean, using eddies database from Chelton et al. (2011) and NCEP–CFRS reanalysis. Moreover, the analysis also allows exploring the characteristic of eddies in the SWA and their fingerprints on heat fluxes.

We found that there is more abundance of cyclonic than anticyclonic eddies in the SWA. The regions where the number of CE is larger are the BMC region, along the mean position of STF and SAF; and at the top of the Zapiola Drift. Eddies with the largest radii (120–180 km radii) are mainly located between 38°S and 42°S; eddies with the lowest radius (40–50 km radii) are mainly located south of 49°S. While there is no dependence on radius of eddy polarity, AE have slightly largest radius compared with CE. Eddies with amplitudes larger than 24 cm are found in regions of high EKE values while in regions with low or moderate EKE the amplitude of eddies is <9 cm. In general, our results for the eddy identification and characterization of the main eddy parameters such as radius and amplitude are in good agreement in comparison with findings from other authors (e.g. Chelton et al. 2007, 2011; Souza et al. 2011; Gaube et al. 2013).

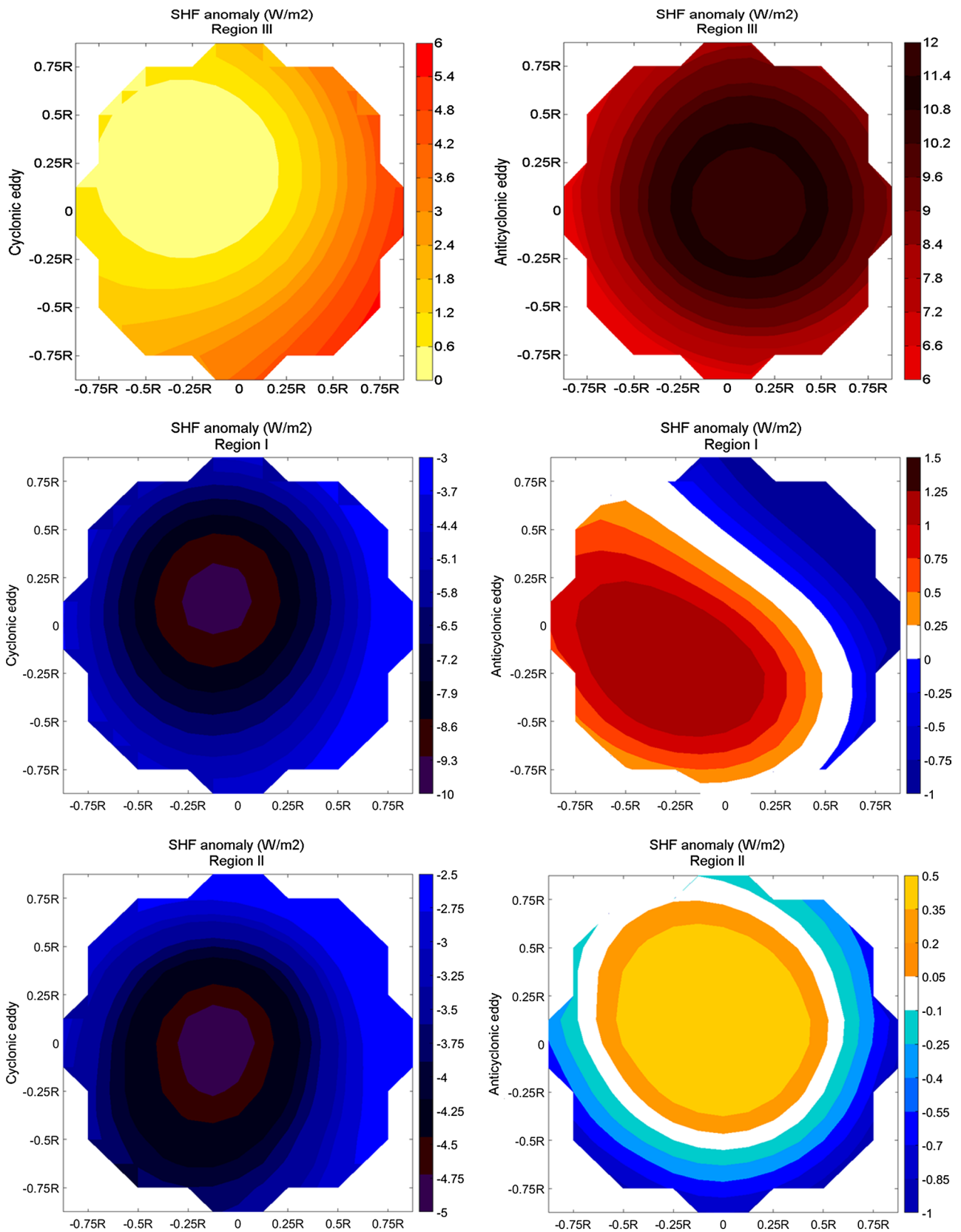


Fig. 6 Composite average of sensible heat flux (W/m^2) inside CE and AE eddies. Eddies are normalized and averaged from NCEP-CFSR (30 km, 6 h) for the period 1992–2010 for eddies over the Bra-

zil–Malvinas Confluence region, subtropical region and the subpolar region, respectively. The zonal mean was removed

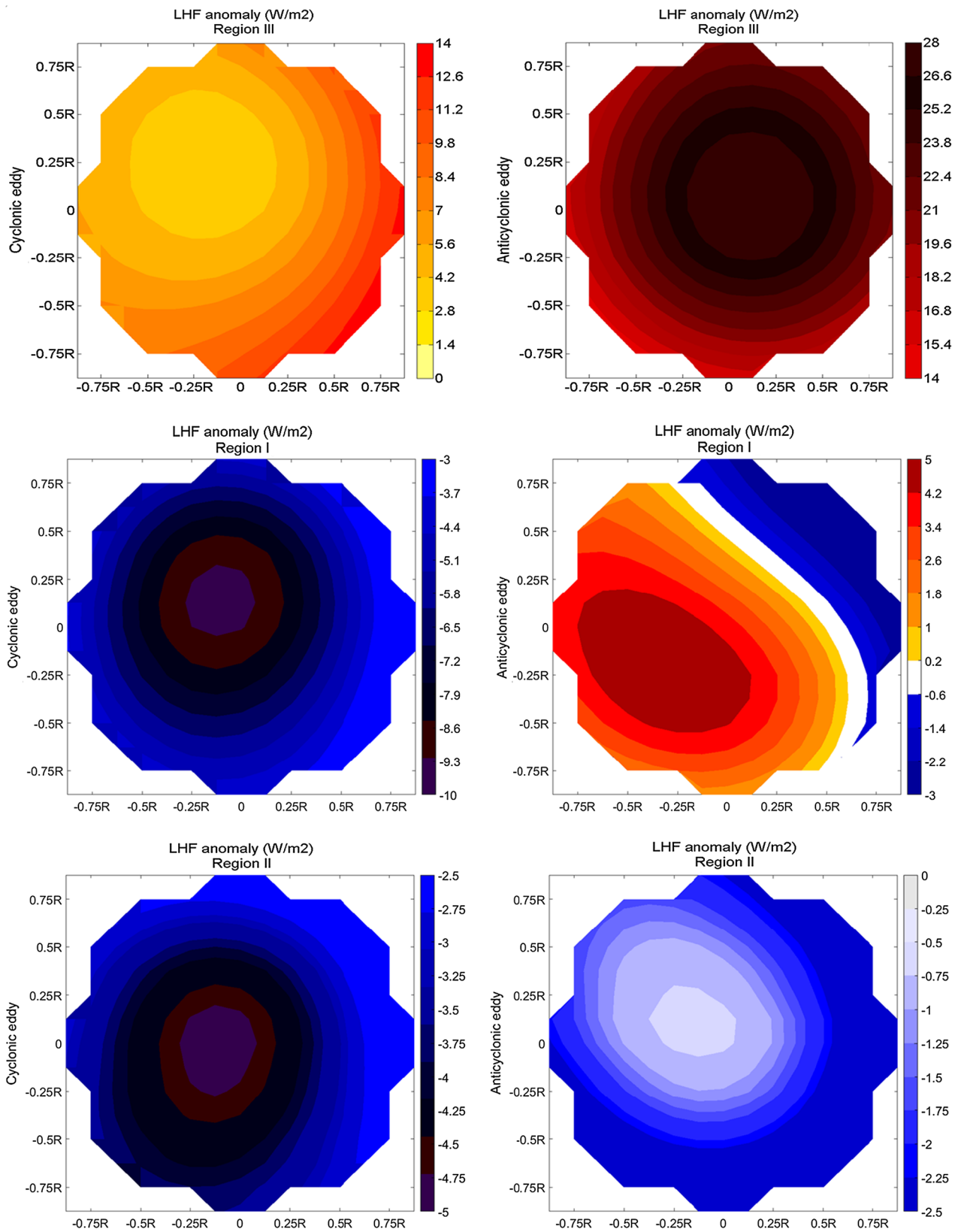


Fig. 7 As Fig. 6 for latent heat flux (W/m^2)

Composite map of eddies showed that the NCEP–CFRSR reanalysis adequately reflects the expected imprint of mesoscale eddies in the SWA: CE have a cold core while AE have warm core. These anomalies could induce enough anomalous heat flux between the ocean and atmosphere. Overall, the pattern of the heat flux imprint by the mesoscale eddies have largest magnitude in the center of the eddy but of opposite sign for AE and CE. AE (CE) causes maximum positive (negative) anomalies with maximum mean anomalies of about $0.5\text{ }^{\circ}\text{C}$ ($-0.5\text{ }^{\circ}\text{C}$) in the SST, 6 W/m^2 (-4 W/m^2) in the SHF and 12 W/m^2 (-9 W/m^2) in the LHF. The largest magnitude of the anomaly is near the eddy center and decays radially outward. The average heat fluxes inside mesoscale eddies are remarkably distinct from the outside, consequently eddies are a great contributor to the SHF and LHF spatial variability. The study presented here only analyzes the surface fluxes. The vertical structure of each eddy will ultimately determine the amount of heat that will be exchanged at the sea surface. However, in situ observations that fully observe an eddy in three dimensions are rare. As far as we know, only one study, combining multi-sensor satellite and in situ measurements, could estimate the three dimensional heat content of a single warm core ocean eddy south of the Brazil–Malvinas Confluence (de Souza et al. 2006). Output from a numerical model should be used to determine if the air-sea fluxes caused by eddies are also modulated by the vertical structure of each eddy.

In the SWA eddies can significantly impact the sensible and latent heat flux variability, affecting the heat exchange at the air-sea interface. Relative contribution in term of eddies to the LHF (SHF) is about 59.5% (51.7%) reaching the maximum observed value at Region III. This asymmetry of heat flux anomalies could locally impact the atmospheric circulation (Hausmann and Czaja 2012; Frenger et al. 2013). However, there is also evidence of air-sea interaction at larger scales, with high and low pressure centers also influencing the SWA: strengthening/weakening of the subtropical high can force fluctuations with a north-south SST dipolar through processes related with the wind and this may have implications on the climate of South America. Diaz et al. (1998) have shown that SST anomalies in the SWA are associated with precipitation anomalies in Uruguay and the southeastern coast of Brazil. Barros et al. (2000) report a significant correlation between warm SST anomalies in the South Atlantic and precipitation in southeastern South America. The principal mode of internal variability at interannual timescales shows a strengthening (weakening) of the South Atlantic convergence zone accompanied by a decrease (increase) of precipitation in southern Brazil, Uruguay and northern Argentina (Barreiro et al. 2002). Thus, the role of the relative contribution of the larger and mesoscales process should be considered.

The geographical distribution of heat fluxes anomalies shows stronger sensible and latent heat fluxes anomalies in the SWA in regions of strong currents where large-amplitude eddies are more commonly observed. On top of that, the largest the amplitude of eddies, the largest the anomalous heat fluxes. We found that eddies in BMC (Region III) have a distinct behavior than eddies in the rest of the SWA: CE and AE have both positive anomalies of latent and sensible fluxes. For CE the anomalous fluxes reach values of 20 W/m^2 (70 W/m^2) for the SHF (LHF) and its minimum is found at around 40°S between 42°W and 32°W with values of -40 W/m^2 (-80 W/m^2), respectively. On the contrary, north of 36°S and south of 50°S , weaker anomalies in CE and fewer significant anomalies in AE are found. To better describe this behavior we repeated the mean composite analysis for eddies in three particular regions. We found that the anomalous heat flux is about half or less of the amplitude obtained with the average eddy in Region I and Region II and it is no longer symmetrical. However, the strongest LHF and SHF anomalies in the SWA occur in regions of strong and unstable currents (strongly mixed water) as BMC (Region III). There, CE have positive anomalies of latent and sensible fluxes. A possible explanation for the anomalous imprint of the CE could be due to the fact that the doming of the isopycnals in the center of the CE is not enough to cool surface waters. Indeed we estimated that most (60.6%) of the CE in this region originate within the very warm subtropical waters and propagate southward. On the contrary, when a CE is generated in a region where there are not so large temperature gradients (as regions I and II) the doming of the CE is enough to cool

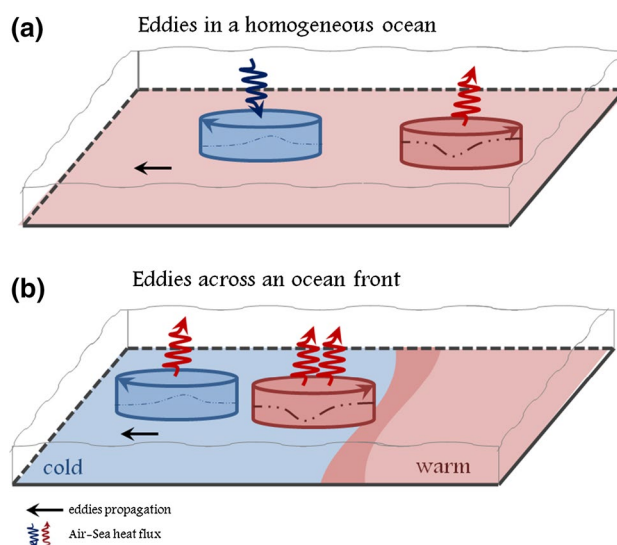


Fig. 8 Schematic summarizing the impact of oceanic eddies in a homogeneous ocean and across an ocean front for an AE (red) and CE (blue)

the sea surface and impact the SHF and LHF. Both situations are schematically represented in Fig. 8. A Lagrangian framework considering the vertical structure of an eddy in the two different environments (large and weak temperature gradients) should be done to corroborate the explanation suggested above.

In summary, our results suggest that mesoscale eddies can affect the lower layers of atmosphere in the SWA. However their imprint depends on the environment where they develop. Consequently, this regional dependence should be taken into account before exploring eddy composites in order to avoid masking out the eddy imprint.

Acknowledgements This work has been supported by the following Grants: FONCyT—PICT-2012-1972, EUMETSAT/CNES DSP/OT/12-2118, ANPCyT PICT 2012-0467, CONICET PIP 112-20110100176, PIO 133-20130100242 and MinCyT/CONAE-001. The authors also thank two anonymous reviewers whose comments greatly helped to improve the manuscript.

References

- Barreiro M, Chang P, Saravanan R (2002) Variability of the South Atlantic convergence zone simulated by an atmospheric general circulation model. *J Clim* 15(7):745–763
- Barros V, Gonzalez M, Liebmann B, Camilloni I (2000) Influence of the South Atlantic convergence zone and South Atlantic Sea surface temperature on interannual summerrainfall variability in Southeastern South America. *Theor Appl Climatol* 67(3–4):123–133
- Byrne D, Papritz L, Frenger I, Münnich M, Gruber N (2015) Atmospheric response to mesoscale sea surface temperature anomalies: assessment of mechanisms and coupling strength in a high-resolution coupled model over the South Atlantic*. *J Atmos Sci* 72(5):1872–1890
- Cayan DR (1992) Latent and sensible heat flux anomalies over the northern oceans: driving the sea surface temperature. *J Phys Oceanogr* 22(8):859–881
- Chelton DB (2005) The impact of SST specification on ECMWF surface wind stress fields in the eastern tropical Pacific. *J Clim* 18:530–550. doi:10.1175/JCLI-3275.1
- Chelton DB (2013) Ocean-atmosphere coupling: mesoscale eddy effects. *Nat Geosci* 6:594–595. doi:10.1038/ngeo1906
- Chelton DB, Xie S (2010) Coupled ocean-atmosphere interaction at oceanic mesoscales. *Oceanography* 23(4):52–69. doi:10.5670/oceanog.2010.05
- Chelton DB, Schlax MG, Witter DL, Richman JG (1990) Geosat altimeter observations of the surface circulation of the Southern ocean. *J Geophys Res* 95(C10):17877–17903
- Chelton DB, Schlax MG, Samelson RM, de Szoeke RA (2007) Global observations of large oceanic eddies. *Geophys Res Lett* 34(15):L15606. doi:10.1029/2007GL030812
- Chelton DB, Schlax MG, Samelson RM (2011) Global observations of nonlinear mesoscale eddies. *Prog Oceanogr* 91(2):167–216
- de Souza RB, Mata MM, Garcia CA, Kampel M, Oliveira EN, Lorenzetti JA (2006) Multi-sensor satellite and in situ measurements of a warm core ocean eddy south of the Brazil–Malvinas Confluence region. *Remote Sens Environ* 100(1):52–66
- Diaz AF, Studzinski CD, Mechoso CR (1998) Relationships between precipitation anomalies in Uruguay and southern Brazil and sea surface temperature in the Pacific and Atlantic Oceans. *J Clim* 11(2):251–271
- Frenger I, Gruber N, Knutti R, Munnich M (2013) Imprint of Southern Ocean eddies on winds, clouds and rainfall. *Nat Geosci*. doi:10.38/ngeo1863
- Gaube P, Chelton DB, Strutton PG, Behrenfeld MJ (2013) Satellite observations of chlorophyll, phytoplankton biomass, and Ekman pumping in nonlinear mesoscale eddies. *J Geophys Res Oceans* 118:6349–6370. doi:10.1002/2013JC009027
- Gordon AL (1981) South Atlantic thermocline ventilation. *Deep Sea Res I Oceanogr Res Pap* 28(11):1239–1264
- Hausmann U, Czaja A (2012) The observed signature of mesoscale eddies in sea surface temperature and the associated heat transport. *Deep Sea Res I Oceanogr Res Pap* 70:60–72
- Klein P, Lapeyre G (2009) The oceanic vertical pump induced by mesoscale and submesoscale turbulence. *Annu Rev Mar Sci* 1:351–375
- McGillicuddy DJ, Robinson AR (1997) Interaction between the oceanic mesoscale and the surface mixed layer. *Dyn Atmos Oceans* 27:549–574
- Nardelli BB (2013) Vortex waves and vertical motion in a mesoscale cyclonic eddy. *J Geophys Res Oceans* 118(10):5609–5624
- Piola AR, Gordon AL (1989) Intermediate waters in the southwest South Atlantic. *Deep Sea Res A* 36:1–16
- Saha S, Moorthi S, Pan HL, Wu X, Wang J, Nadiga S et al (2010) The NCEP climate forecast system reanalysis. *Bull Am Meteorol Soc* 91(8):1015
- Samelson RM, Skillingstad ED, Chelton DB, Esbensen SK, O’Neill LW, Thum N (2006) On the coupling of wind stress and sea surface temperature. *J Clim* 19(8):1557–1566
- Saraceno M, Provost C (2012) On eddy polarity distribution in the Southwestern Atlantic. *Deep Sea Res I* 69(11):62–69
- Saraceno M, Provost C, Piola AR, Bava J, Gagliardini A (2004) Brazil Malvinas Frontal System as seen from 9 years of advanced very high resolution radiometer data. *J Geophys Res Oceans* 109:C05027. doi:10.1029/2003JC002127
- Saraceno M, Provost C, Zajaczkovski U (2009) Long-term variation in the anticyclonic ocean circulation over the Zapiola Rise as observed by satellite altimetry: evidence of possible collapses. *Deep Sea Res I Oceanogr Res Pap* 56(7):1077–1092
- Souza JMAC, De Boyer Montegut C, Le Traon PY (2011) Comparison between three implementations of automatic identification algorithms for the quantification and characterization of mesoscale eddies in the South Atlantic Ocean. *Ocean Sci* 7(3):317–334
- Souza JMAC, Chapron B, Autret E (2014) The surface thermal signature and air–sea coupling over the Agulhas rings propagating in the South Atlantic Ocean interior. *Ocean Sci* 10(4):633–644
- Tilburg CE, Subrahmanyam B, O’Brien JJ (2002) Ocean color variability in the Tasman Sea. *Geophys Res Lett* 29(10):1487. doi:10.1029/2001GL014071
- Trenberth KE, Fasullo JT, Kiehl J (2009) Earth’s global energy budget. *Bull Am Meteorol Soc* 90(3):311
- Villas Bôas AB, Sato OT, Chaigneau A, Castelão GP (2015) The signature of mesoscale eddies on the air–sea turbulent heat fluxes in the South Atlantic Ocean. *Geophys Res Lett* 42(6):1856–1862
- Xie S (2004) Satellite observations of cool ocean-atmosphere interaction. *Bull Am Meteorol Soc* 85:195–208
- Yu L, Weller RA (2007) Objectively analyzed air–sea heat fluxes for the global ice-free oceans (1981–2005). *Bull Am Meteorol Soc* 88(4):2007